Spectroscopic diagnostics and experimental planning for plasma-surface interaction studies in NSTX-U

57th APS-DPP Meeting

Nov. 16-20, 2015
Savannah, Georgia, US

F. Scotti, V.A. Soukhanovskii, A.L.Roquemore,
J.P. Allain, F. Bedoya, C.H. Skinner

Lawrence Livermore National Laboratory

Fusion Energy Sciences

NSTX Upgrade

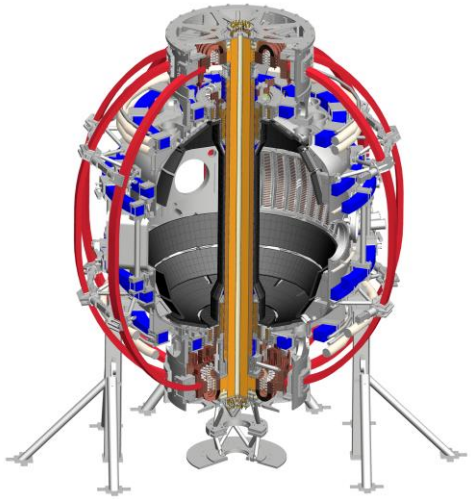

PPPL

U.S. DEPARTMENT OF ENERGY | Office of Science

LLNL-PRES-XXXXXX

This work was performed under the auspices of the U.S. Department of Energy by Lawrence Livermore National Laboratory under Contract DE-AC52-07NA27344. This material is based upon work supported by the U.S. Department of Energy, Office of Science, Office of Fusion Energy Sciences.. Lawrence Livermore National Security, LLC

Abstract & Acknowledgements

In the mixed-material environment of the NSTX-U first wall, a comprehensive set of visible imaging diagnostics will be used to study the evolution of the plasma facing component (PFC) surface conditions and the spatial distribution of impurity influxes. Characterizing the dynamic material environment originating from different wall conditioning techniques (boronization, lithium evaporation) on graphite PFCs requires simultaneous monitoring of emission from different atomic species. Full poloidal/toroidal coverage of impurity emission is achieved via a combination of narrow-bandpass-filtered fast cameras viewing upper and lower divertor PFCs and line-scan cameras. Two image-intensified radiation-hardened charge-injection-device cameras expand these capabilities with the ability to image weaker visible lines and a custom-built two-color system for the simultaneous imaging of different wavelengths on the same detector. Intensified camera views include the lower divertor and a close-up of the surface analysis sample system Material Analysis and Particle Probe (MAPP). Redundant views via multiple cameras and two-color setups will enable a more accurate determination of impurity influxes (via line ratio techniques) and the simultaneous characterization of carbon (chemical/physical), lithium and oxygen influx evolution following lithium and boron wall conditioning.

Supported by U.S. DOE Contracts: DE-AC02-09CH11466, DE-AC52-07NA27344.

With acknowledgements to J. Dong, G. Zimmer, W. Davis, S. Kampel, K. Tindall

Boronization, lithium evaporation will be the conditioning methods for NSTX-U graphite PFCs

- Graphite is the main PFC material in NSTX
  - ATJ tiles on divertor and outer wall
  - ATJ and POCO tiles on center stack, neutral beam dump
  - High-Z tile upgrade (single row) during 2016 outage
- Full vessel bake at 350°C, D+He GDC
- Boronization via D-TMB bled in during He-GDC
- Lithium conditioning via lithium evaporators
  - Toroidally asymmetric
  - 100-300 mg between discharges (~10^{21} atoms/m^2)

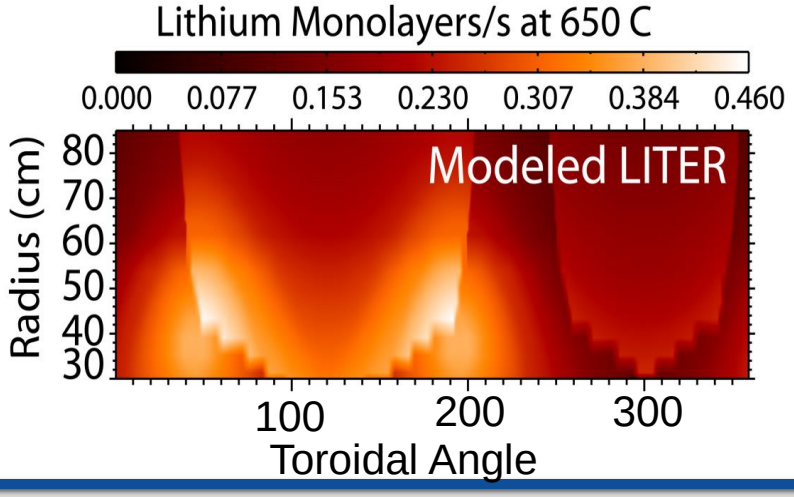

The NSTX-U first wall will effectively be a mixed material environment (C, B, Li, O)

- Boronization, lithium evaporative coatings, lithium intercalation in graphite, oxygen gettering by C-Li compounds will make the NSTX-U first wall a mixed material environment
- Evolution of C, B, Li, O sources with Li introduction not fully understood
  - Reduction in C sputtering observed after large lithium deposition
  - Lithium sputtering consistent with physical and thermal sputtering from D-saturated lithium
- Past experiments indicate need for:
  - Simultaneous monitoring of emission from multiple elements
  - Surface science and connection of surface science with spectroscopy

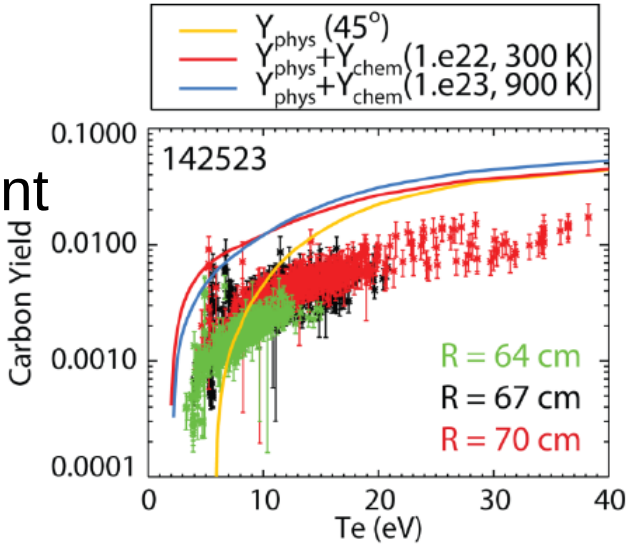

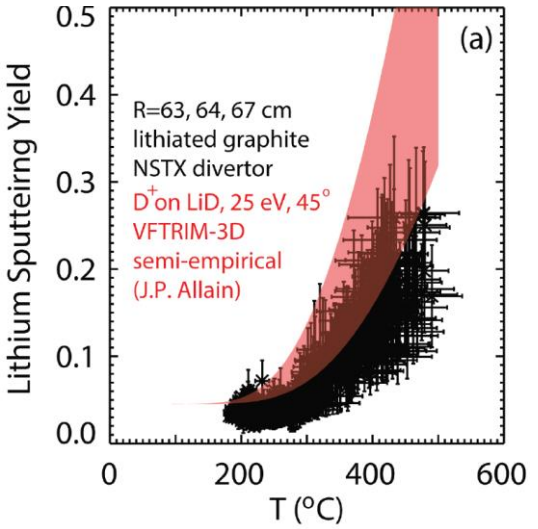

Wall conditioning via lithium coatings in NSTX resulted in carbon accumulation

- Lithium conditioning led to suppression of ELMs:
  - Carbon inventory increased by 3-4X
  - Low core lithium density (n_{Li}/n_e<0.1%)
  - High-Z impurity accumulation led to core P_{rad} up to 50% of P_{inj}
- Carbon inventory increase attributed to ELM disappearance, weaker impurity screening, unknown role of wall sources
- Indicated need for better poloidal coverage of impurity emission, n_e, T_e to determine impurity influxes and understand carbon balance

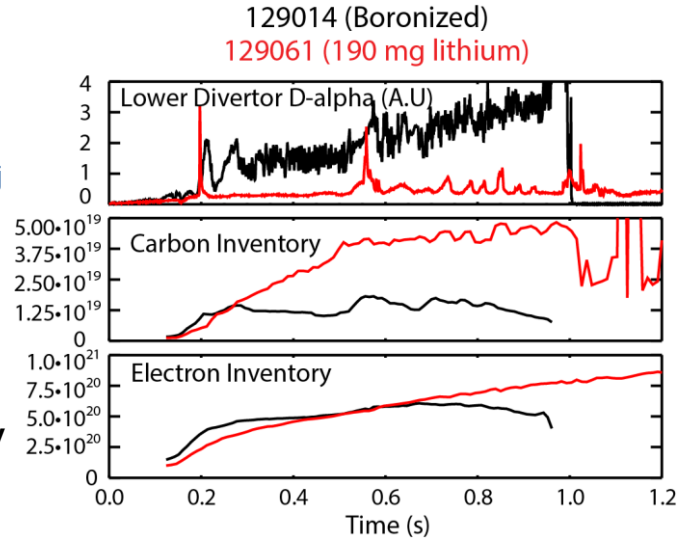

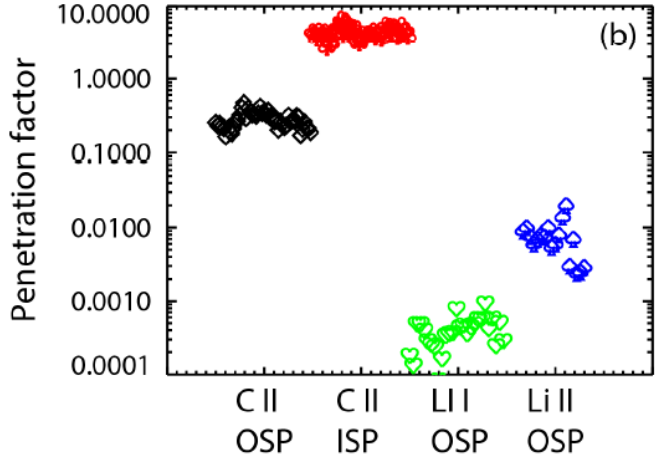

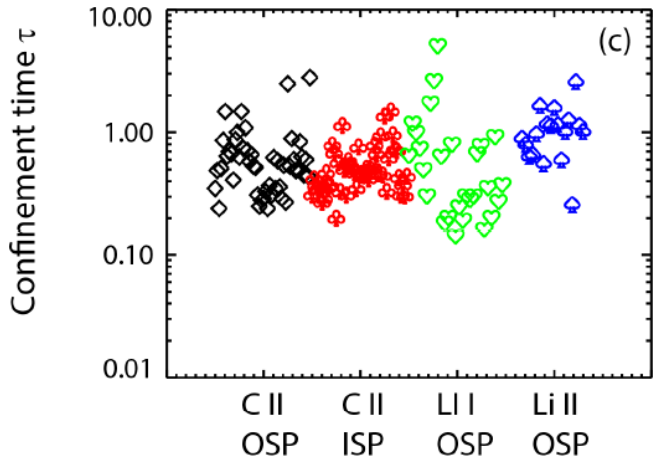

Toroidal asymmetries in impurity influx observed in NSTX, possibly important for impurity balance

- Toroidally-asymmetric lithium influxes observed following lithium deposition profile in NSTX
  - Temperature-enhanced sputtering, droplet ejection?
- Tile-to tile misalignment evident on NSTX CS, divertor tiles, led to tile edges effects and enhanced carbon influxes
- New tiles installed with emphasis on tile-to-tile alignment
- Indicated need for:
  - Full toroidal coverage of divertor PFCs to evaluate asymmetries in carbon/lithium influxes due to boronization, lithium-conditioning
  - Radial view to determine effects of tile-misalignment on carbon sources

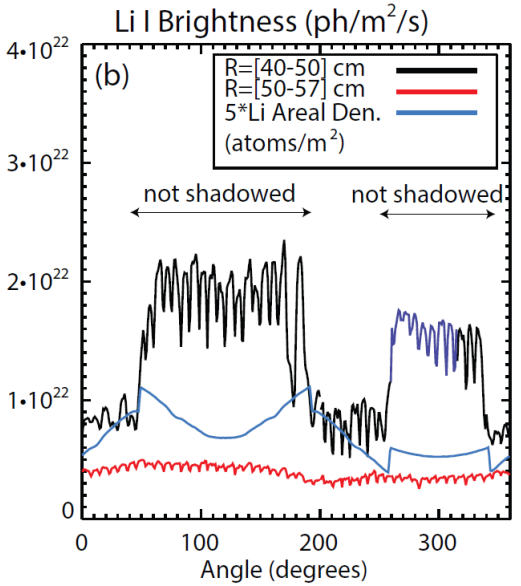

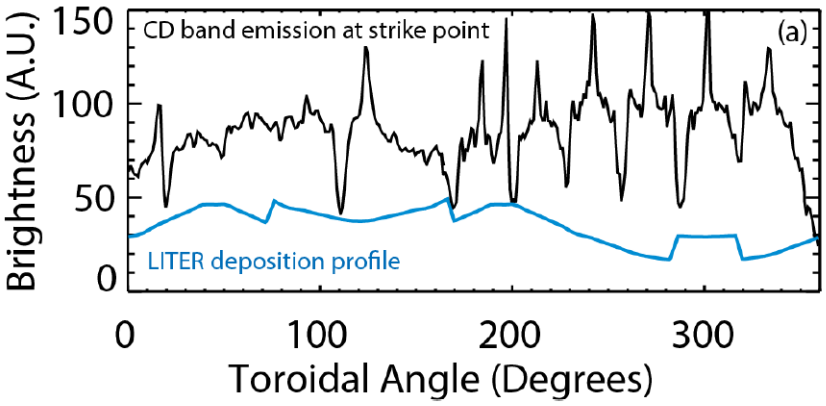

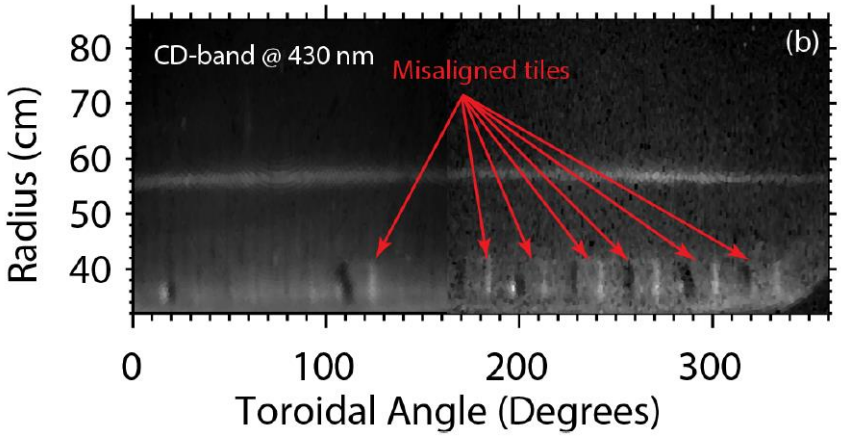

Toroidally asymmetric PMI observed in NSTX due to 3D fields, RF heating, ELMs

- Application of 3D magnetic perturbations can result in OSP splitting in helical lobes
- ELMs can result in non-axisymmetric deposition of particle and heat fluxes
- RF heating in NSTX results in power coupled to the edge → non-axisymmetric divertor power deposition
- Indicated need for:
  - Full toroidal coverage of divertor PFCs to evaluate asymmetries in divertor particle fluxes

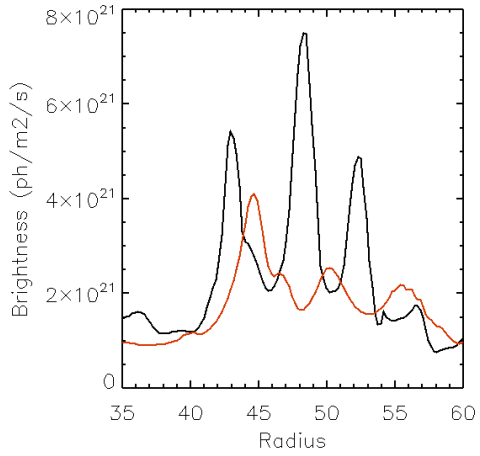

Phi=120º

Phi=180º

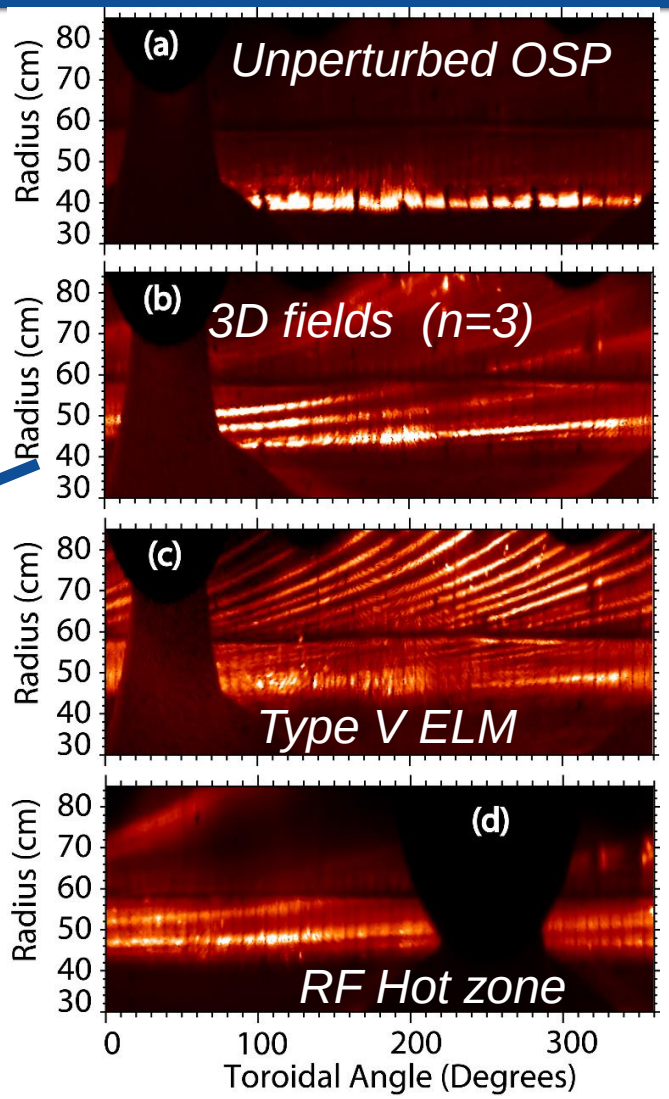

Goal: Evaluation of impurity sputtering, influxes, particle balance with boronized and lithiated PFCs

- Enhanced spectroscopic imaging diagnostic suite to enable:
  - Full toroidal/poloidal coverage of impurity emission
  - Simultaneous measurements of impurity brightness from different atomic elements
  - Redundant measurements of impurity brightness from different wavelength of same impurity charge state

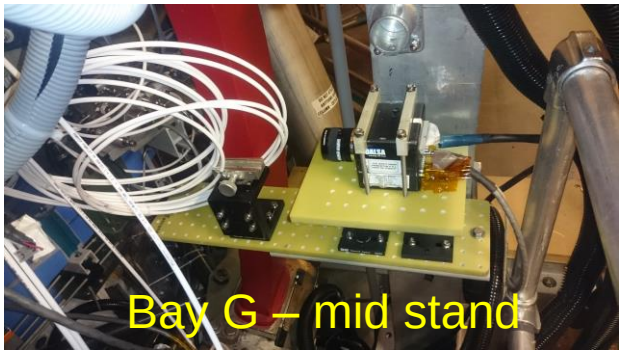

Tools: Upgraded diagnostics for full poloidal, toroidal coverage of impurity emission

- Full poloidal coverage of impurity emission + full toroidal divertor coverage
  - Phantom (4), CIDTEC (2 two-color), DALSA (1), 1D-CCD (9) cameras, 3 spectrometers
- High resolution views for MAPP and inboard divertor
- View of the NBI armor tiles (ENDD-U)
- Views centered at probes toroidal location
- Availability/reliability of probes limited extrapolation of influxes
  - Redundant wavelength approach implemented for FY2015

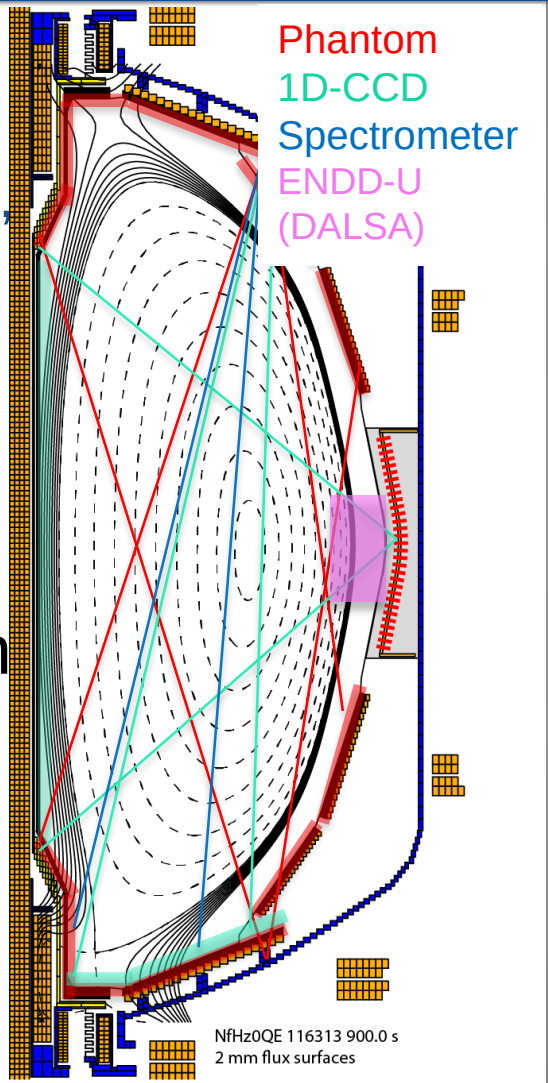

Tools: Upgraded diagnostics for full poloidal, toroidal coverage of impurity emission

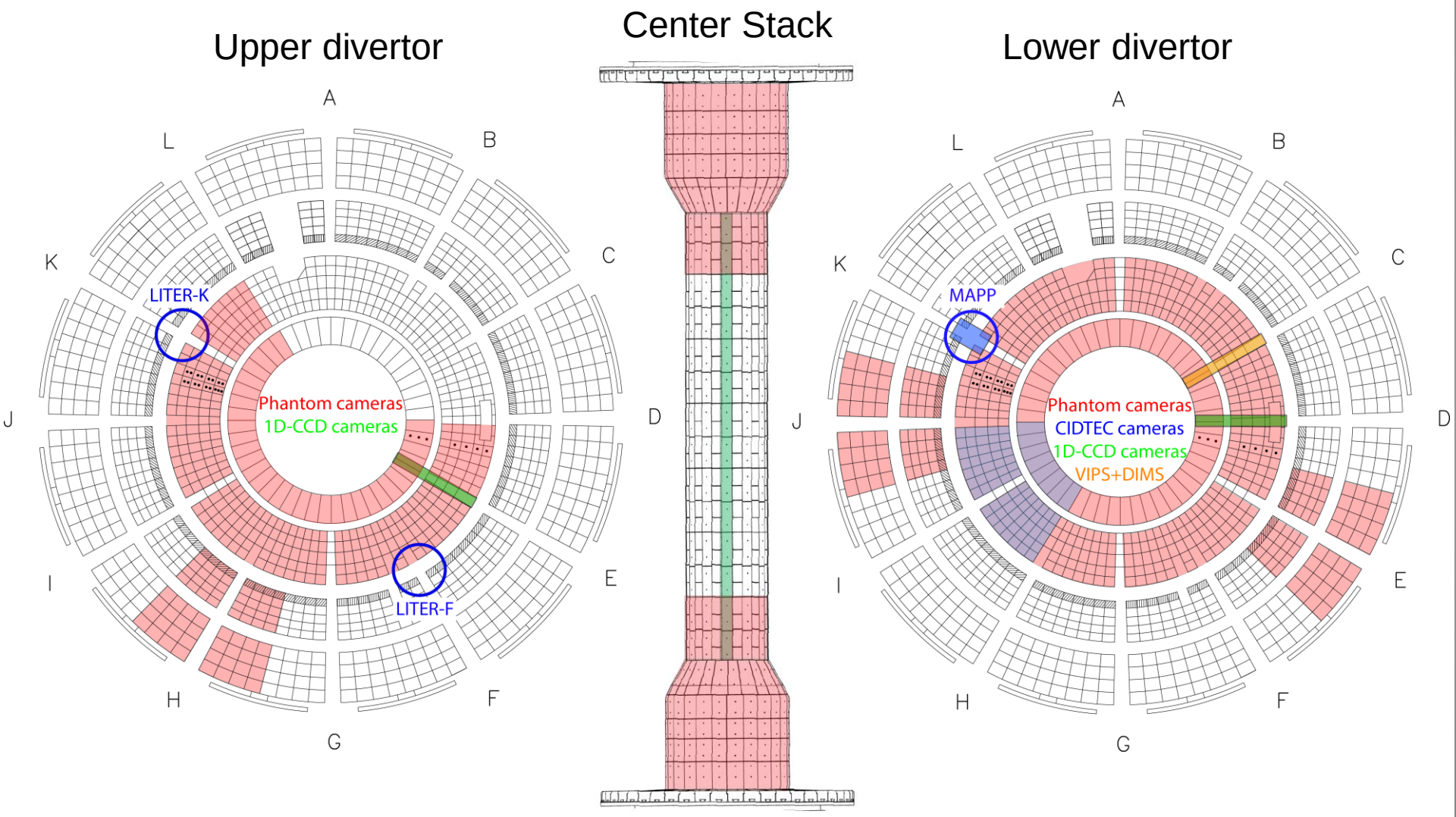

Strategy: Simultaneous monitoring of different lines for divertor impurity influxes

- Simultaneous measurement of multiple lines of same charge state (carbon and lithium) to avoid uncertainty in plasma parameters (T_e, n_e) in lower divertor
  - C II lines with different dependencies on plasma parameters
    → C^{1+} influx determination (426, 514, 723 nm) via S/XB method
  - Li I lines with different dependencies on plasma parameters
    → Li^{0+} influx determination (460, 610, 670 nm) via S/XB method
  - Gerö band (CD) + C II line + D-γ
    → Chemical vs physical sputtering contribution
  - 909 nm region (DIMS)
    → C^{0+} influx, complementary evaluation of f_{chem}/f_{phys}
- Upper divertor views to inform on evolution of upper PFCs

Diagnostic set to also support turbulence, surface science, impurity injection studies, divertor control

- Dedicated view on Bay J top for the Material Analysis and Particle Probe (MAPP) for comparison of elemental composition from surface science and spectroscopy
- Dedicated view on Bay J midplane to support Supersonic Gas Injector (SGI), Lithium Granule Injector (LGI) and Laser Blow-Off (LBO) experiments (2017)
- Fast framing rates up to 200 kHz (on restricted FOV) to support turbulence studies via correlation to midplane Gas Puff Imaging (GPI)
- 10 Gb/s connection on new Phantom to support real-time radiative divertor control via radial divertor port

Two dimensional fast cameras were installed with full toroidal/poloidal coverage of NSTX-U PFCs

- Two re-entrant view ports on top ports separated by 150°, one on bottom port
  - 8”-long pipe, 3.5” diameter, 3” sapphire window
  - Enable:
    - Full toroidal coverage of lower divertor PFCs
    - Over half toroidal coverage of upper divertor PFCs
    - Full poloidal coverage of PFCs at a single toroidal location
  - Remotely-operated pneumatic shutters protect windows from lithium coatings

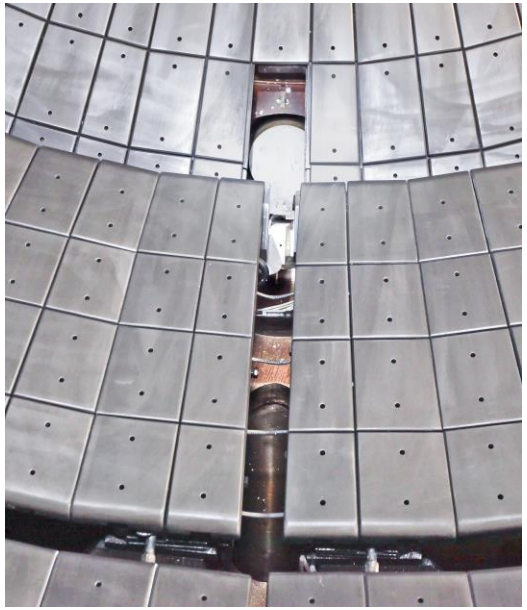

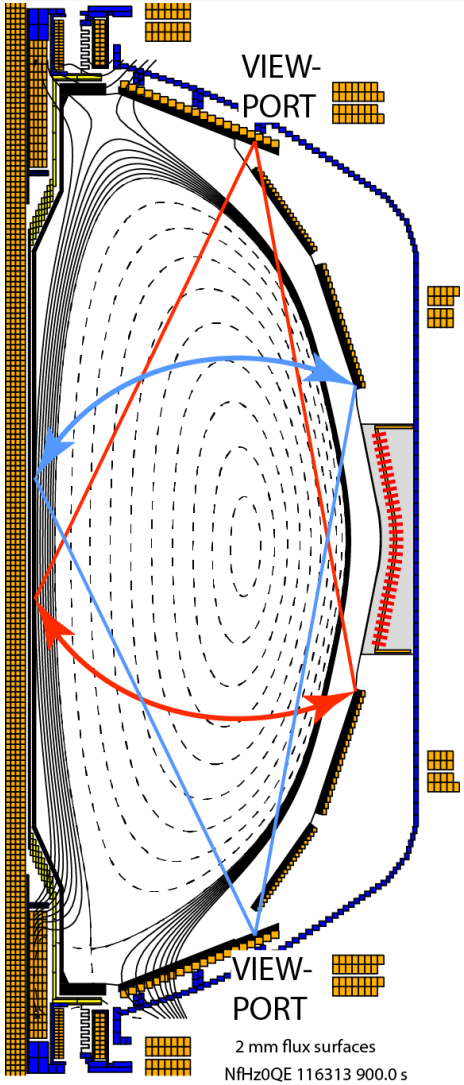

Wide angle view, small center stack radius allow full divertor toroidal coverage with two cameras

- Each camera covers over 180º toroidally
- Typical resolution of ~ 256x208 pixels gives spatial resolution better than 1cm/pixel allowing fast framing rates
- Fast optics, fast framing detectors and narrow bandpass filters allow studies of impurity emission, non-axisymmetric effects, turbulence

Lower divertor view (Bay E) Lower divertor view (Bay J) Upper divertor view (Bay H)

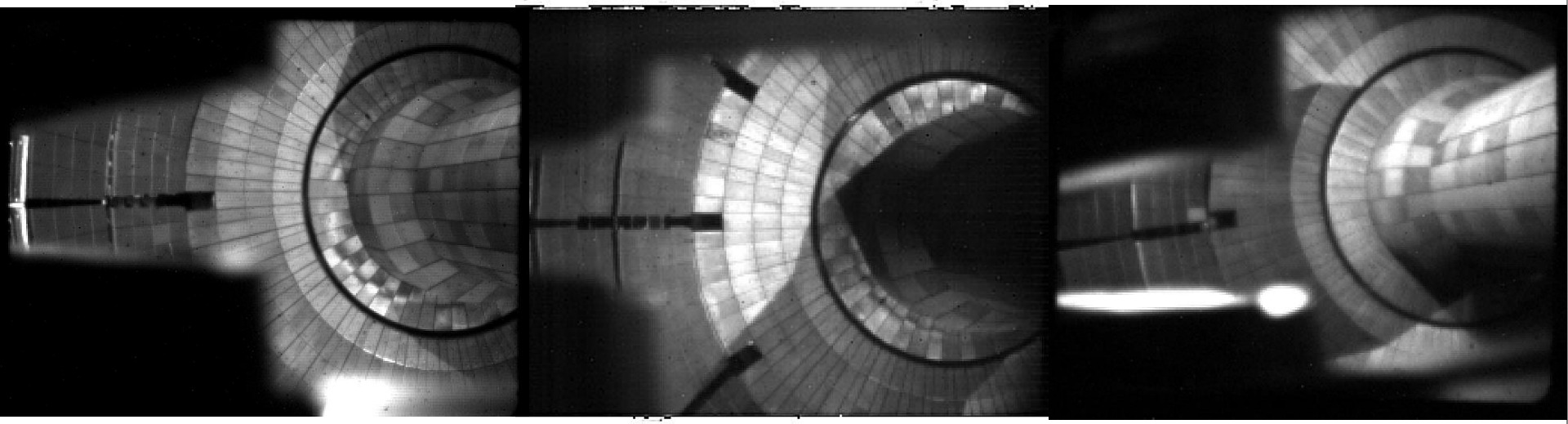

Fast optics, imaging bundles and bandpass filters for high-resolution imaging at fast framing speed

- Collection optics:
  - f=16mm, F/1.4, 2/3” format C-mount lens (Pentax) → 44º wide angle view,
- Collected light imaged on coherent optical fiber bundle:
  - 15’-long, 1000x800 10µm fibers, Schott IG-163
- Collimating optics:
  - f=100mm, F/2.8, 2/3” format C-mount lens (Kowa)
  - f=75mm, F/1.4, 2/3” format C-mount lens (Pentax)
- Focussing optics:
  - f=50mm, F/1.4, 2/3” format, C-mount lens (Pentax)
  - Demagnification to fill ~1/16 of the sensor area

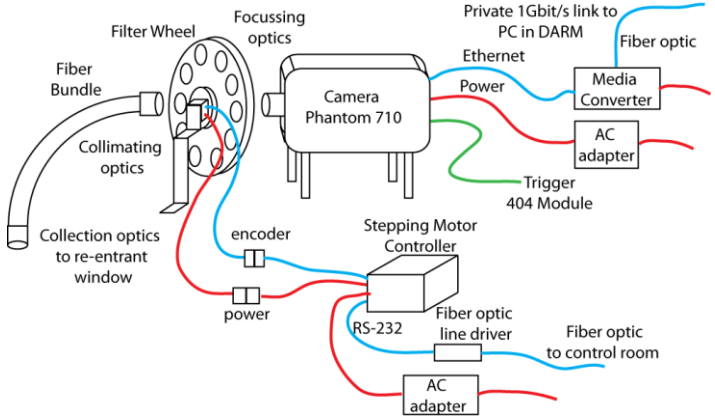

- Bandpass filters:
  - Narrow bandpass filters (2”, 1.5 nm FWHM, ANDOVER) on remotely controlled filter wheel
  - Multiple wheels on Ethernet-addressable RS-232 server

High quantum efficiency, high dynamic range fast framing rate Vision Research CMOS cameras

- Vision Research Phantom v710:
  - 1280x800 pixels sensor, 25.6x16.0 mm area (20 µm pixel)
  - 12 bit dynamic range, max. acquisition speed of 100kfps at 256x208 pixels
- Vision Research Phantom v7.3:
  - 800x600 pixels sensor, 17.6 x 13.2 mm area (22 µm pixel)
  - 14 bit dynamic range, max. acquisition speed of 60kfps at 224x184 pixels
- Vision Research Miro 4:
  - 800x600 pixels sensor, 17.6 x 13.2 mm area (22 µm pixel)
  - 12 bit dynamic range, max. acquisition speed of 10kfps at 224x184 pixels

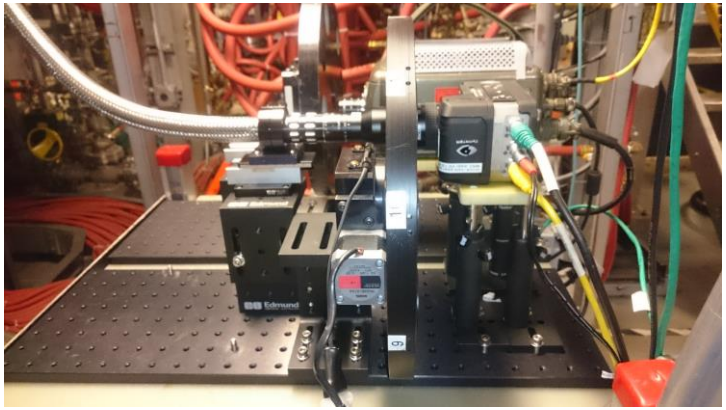

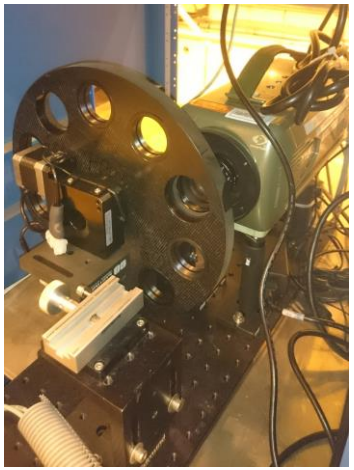

Toroidal remapping enables easier analysis of non-axisymmetric plasma material interaction

- Toroidal remapping of divertor camera images performed via ellipse fitting of divertor surfaces [Scotti, RSI 2012]
- Enables analysis of non-axisymmetric effects
  - Strike point splitting due to 3D fields
  - Toroidal asymmetries in impurity sources
  - Edge filaments footprints
  - RF spirals

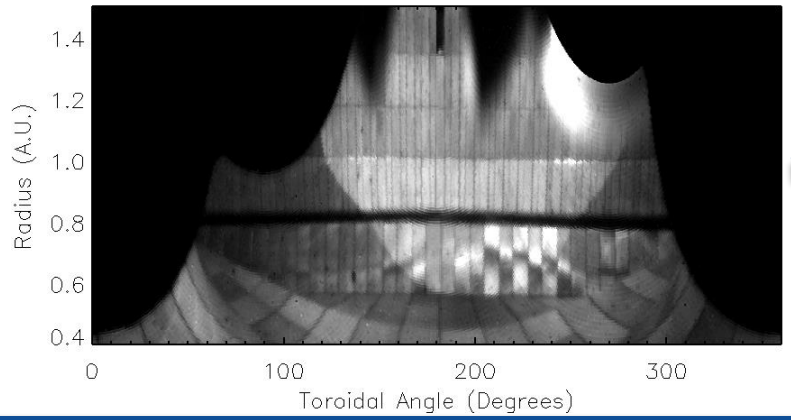

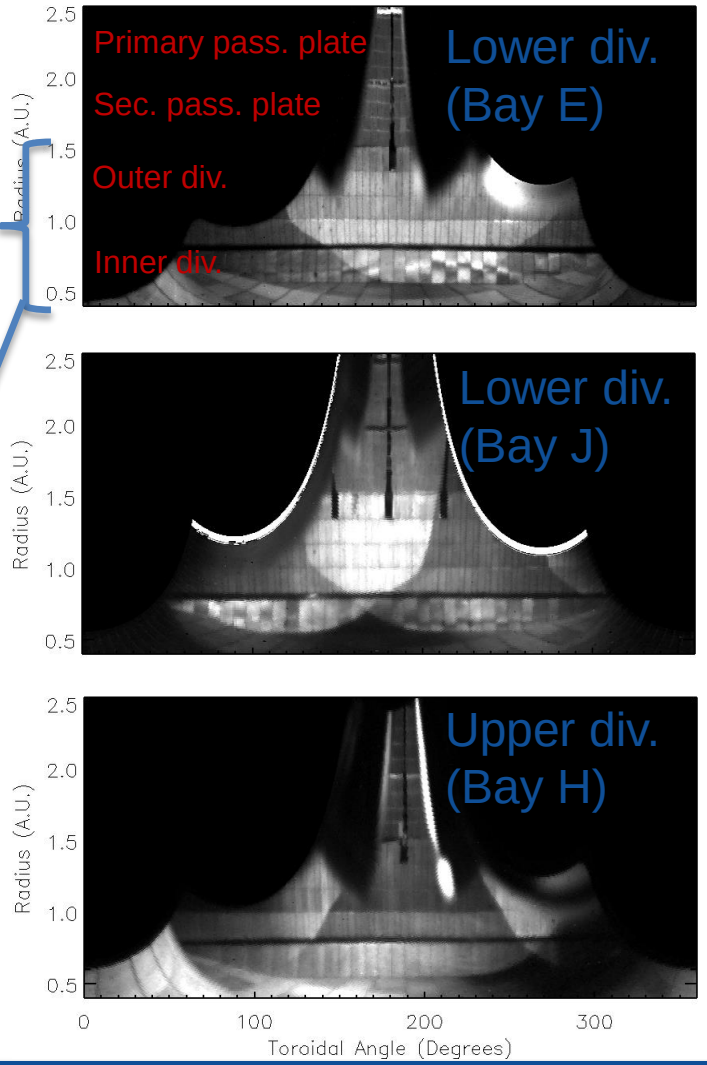

Intensified radiation-hardened CID cameras to complement fast cameras capabilities

- Charge Injection Device (CID) cameras have been used in DIII-D (Groth RSI 2009) and C-Mod (James PPCF, 2013) for hydrogen, impurity emission, erosion studies
- Two CID cameras (ThermoScientific) now installed on NSTX-U:
  - Equipped with image intensifier and UV-sensitive
    - Integrate visible imaging with capability for low intensity and UV lines (direct imaging)
    - Ideal for O, B, Mo, W erosion with either weak visible lines or UV lines
  - Beam splitter optics for two-color capability on same detector
    - Different charge states of same impurity (e.g., lithium gross vs net erosion)
    - Measurement of impurity influx independent from local parameters from line ratio of different lines from same charge state (e.g., Li I)
    - Line ratio measurements for T_e, n_e determination (e.g., Li I 670, 610, 460 nm)
    - Understand role of oxygen in regulating lithium behavior with simultaneous monitoring of O and Li emission
    - Simultaneous imaging of chem. vs phys. carbon sputtering yield

Two-Wavelength Imaging Camera Equipment-1 (TWICE-1) system

- ThermoScientific CIDTEC camera CID8710D1M:
  - VGA resolution (720x480) – 8 bit - 12x13 micron pixel
  - Image intensifier (Photonis GENII-UV, P43 phosphor)
  - 30 Hz interlaced RS-170 analog output
  - External Pleora frame grabber for GigE Vision compliant stream
  - Gating adjustable from 20 ns to 16 ms

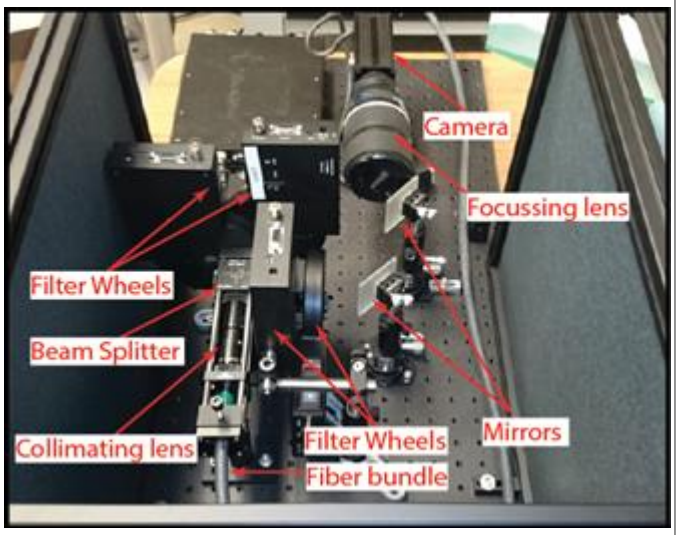

- Beam splitter and remotely-controlled filter wheels for simultaneous 2-color imaging on detector
  - Two wheels for 1” bandpass filters (ANDOVER, FWHM ~1.5 nm)
  - Two wheels for neutral density filters (1.e-3 attenuation)
  - Thorlabs cage mounted components

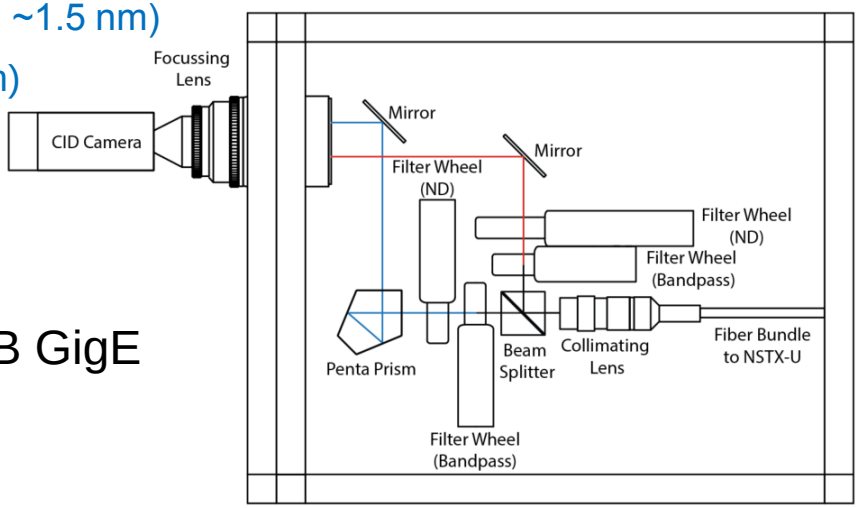

- Python-based data acquisition based on A&B GigE Vision SDK

Collection optics mounted on vessel, image relayed via coherent fiber bundle

- Collection optics in re-entrant viewport: divertor and MAPP view
- Fiber bundle to relay image (Schott, 400x400 10 μm fibers)
- Optics chosen to conserve etendue, minimize vignetting and bandpass shift of interference filters
- Two configurations to fill either horizontal or vertical detector dimension changing collimating optics
- Penta-prism used allows imaging of same area

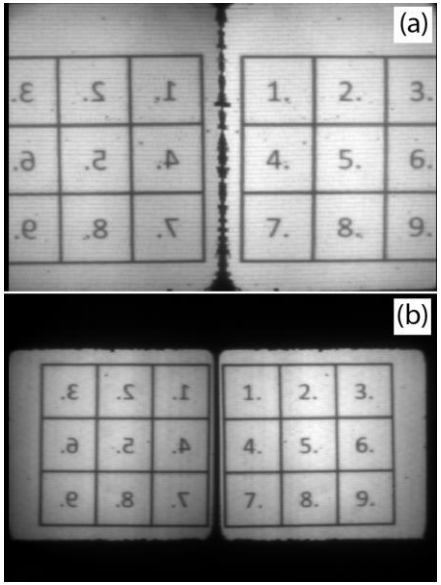

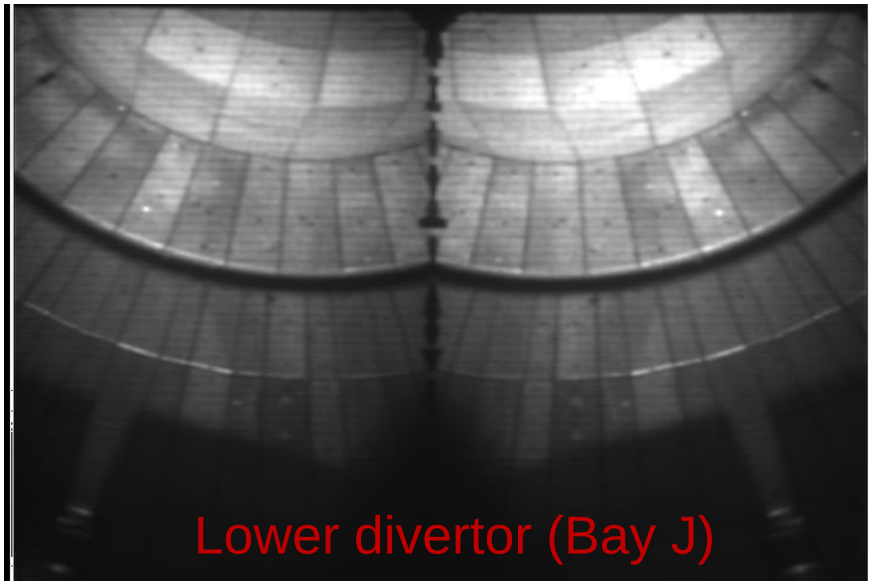

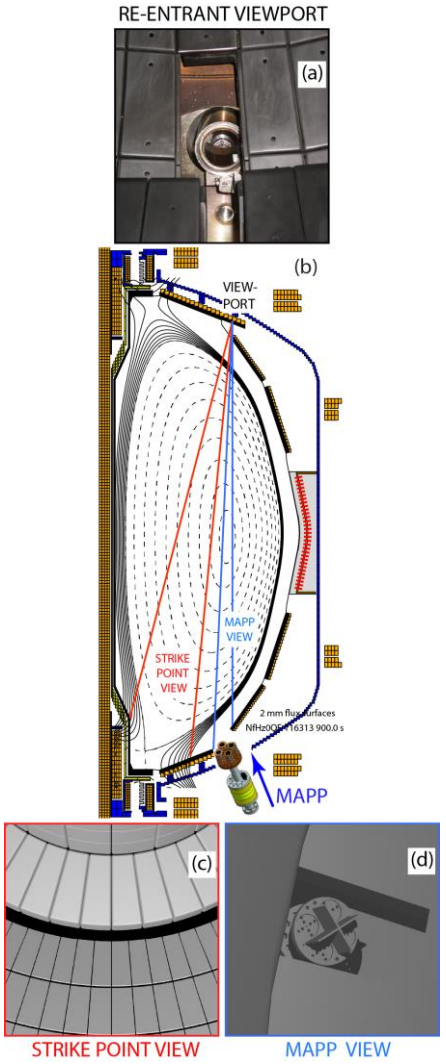

Intensifier and neutral density filters allow imaging of emission lines with differences in emissivity up to 10^3

- Collection, collimating, focusing optics:
  - f=16mm, F/1.4, 2/3” format C-mount lens (Pentax),
  - f=50mm, F/2.3, 2/3” format C-mount lens (Fujinon)
  - f=135mm, F/2.0, full frame format, F-mount lens (Nikkor)
- Bandpass filters:
  - Bandpass filters (1”, 1.5 nm, ANDOVER) on remotely controlled filter wheel on addressable RS-232 server
  - Li I (460, 610, 670 nm), B I (563 nm), B II (703 nm), O II (441.6 nm), CD band (430 nm), C II (514, 426 nm)
- Gain allows for ~ 10^3 intensification, dynamic range degradation beyond digitization level only above gain = 6
- Neutral density filter up to ND 3.0 guided by intensifier gain

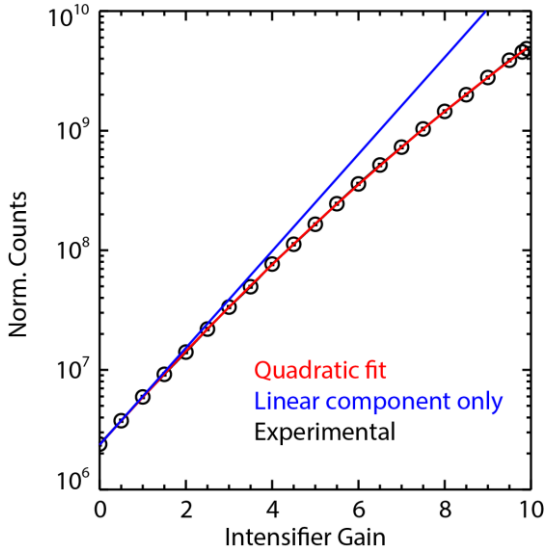

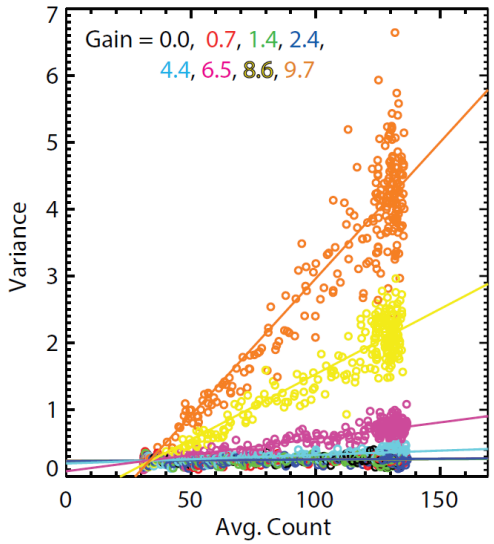

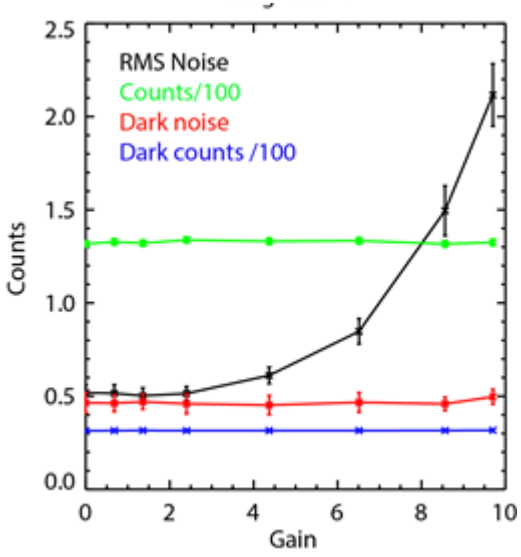

TWICE-2 system for higher throughput via larger bundle, higher-gain intensifier

- ThermoScientific CIDTEC camera CID3710D1M (same detector as 8710)
  - Image intensifier XD-4 S-25 photocathode, P43 phosphor
  - Fiber bundle to relay image (Schott, 1000x800 10 μm fibers)
  - f=35mm, F/1.4, 2/3" format C-mount lens (Pentax),
  - f=100mm, F/2.8, 2/3" format C-mount lens (Kowa)
  - f=105mm, F/2.0, full frame format, F-mount lens (Nikkor)

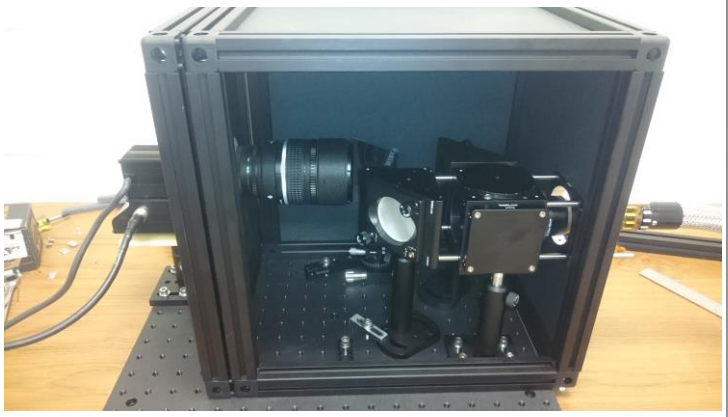

- Beam splitter and fixed filters for 2-color imaging:
  - Thorlabs cage mounted components
  - Dedicated to D-γ and CD Gerö band imaging

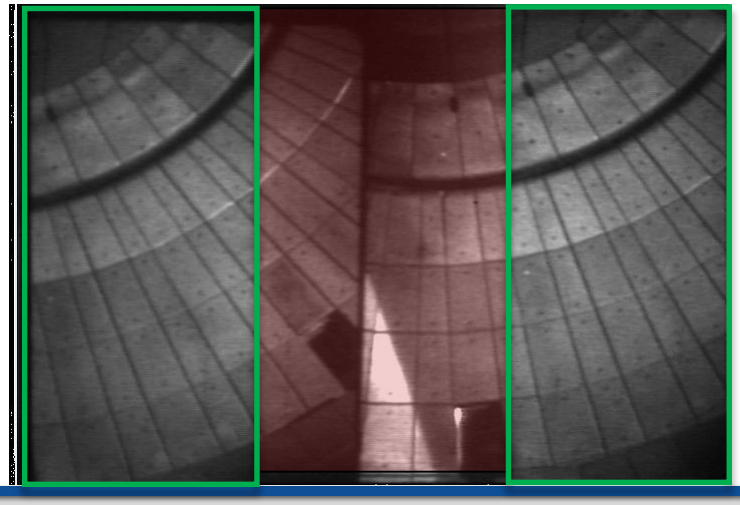

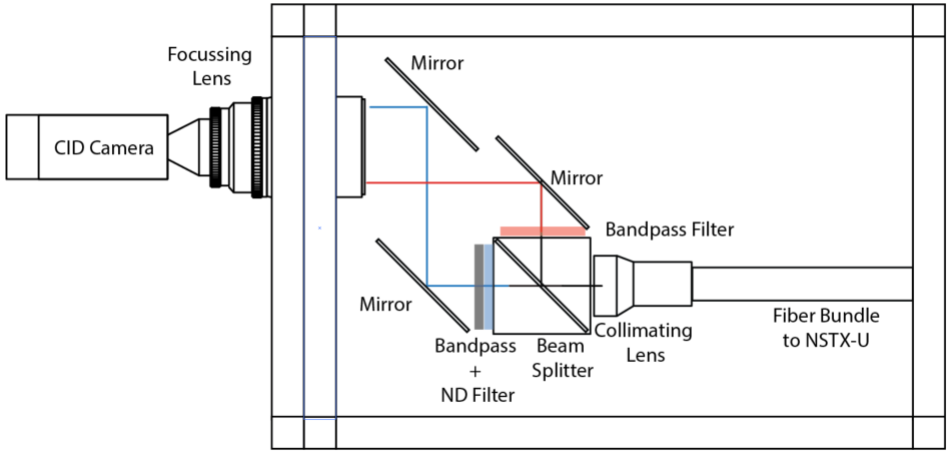

New LLNL Phantom v1211 dedicated to divertor turbulence, divertor control, LGI imaging

- New Vision Research Phantom v1211 camera
  - 1280x800 pixels, 28μm pixels, 12 bit
  - 5 times higher sensitivity wrt Phantom v710
  - 12 kHz @ full frame, 24GB memory, 10 Gbs Ethernet output
- Coherent fiber bundle 1000x800 10 μm fibers, 15' long
- 1:1 imaging on detector:
  - Collimating f=85 mm, F/1.4, Nikkor
  - Focussing f=85 mm, F/1.4, Nikkor
  - 3" bandpass filter
- Resolution:
  - 360x288 pixels (crop 360x100)
- Max fps:
  - 76.6kHz (crop 182.7kHz),
- Max. recording time:
  - 2s

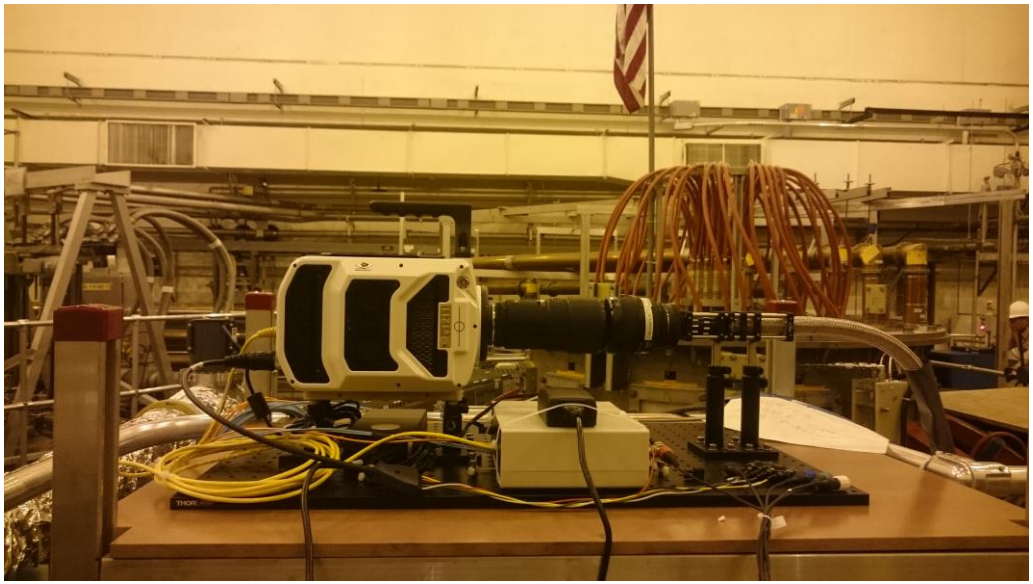

Divertor views from midplane and radial divertor ports for turbulence studies, radiative divertor control

- Two setups will be used for turbulence studies and radiative divertor control
  - Midplane port (6” flange) on Bay J port cover
  - Radial divertor port (2” window) on Bay B lower dome
- Support divertor turbulent filaments characterization (via D-α, Li I filters) for cross correlation with midplane blobs (GPI)
  - Framing rates above 100 kHz typically easily achievable via Li I emission
- Support radiative divertor control via imaging of carbon ionization front (via C III filter)
  - Expected signal would allow ~10 kHz imaging of C III 465 nm emission line

Lower divertor from Bay J mid

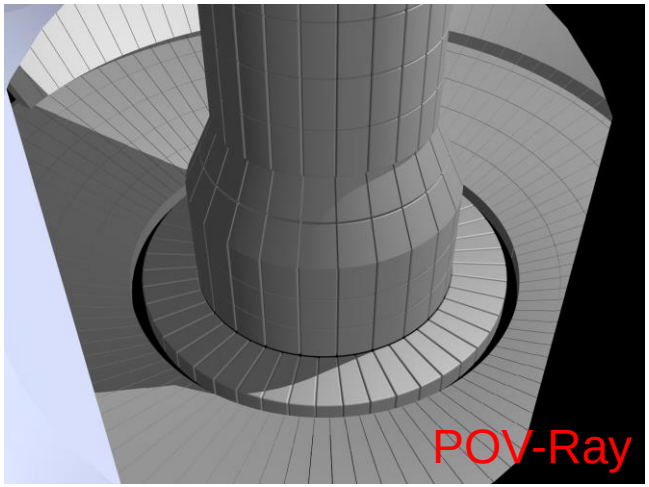

Radial divertor view from Bay B lower dome

Previous implementation in NSTX (D-α)

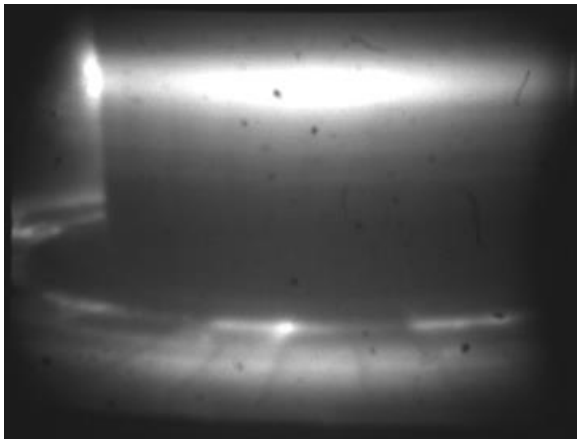

New Phantom camera to support granule injection experiments via imaging of granule ablation cloud

- 12 o'clock port (6" flange) on Bay J midplane
- Lines of sight do not intersect divertor legs
- Candidate imaging filters (Li I – II, C I – II, B I – II, W I, Mo I) according to granule material
- Field of view (~18 cm) allows outer gap variations, 0.5mm/pixel resolution

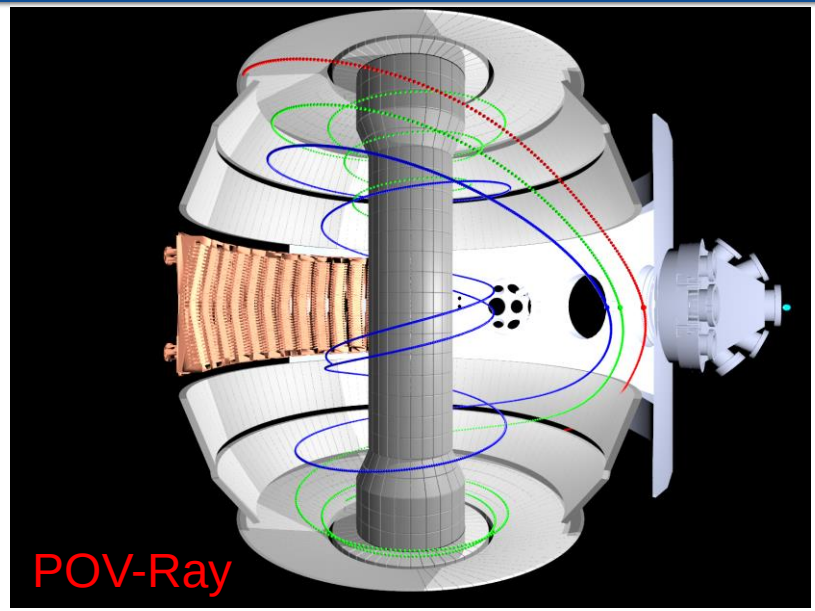

Rendered field of view (POV-Ray) with imaging bundle and 50 mm lens

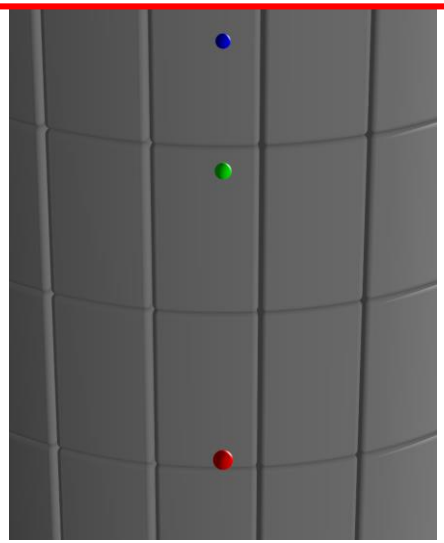

3 granules:

Ψ_N=0.6

Separatrix

Limiter

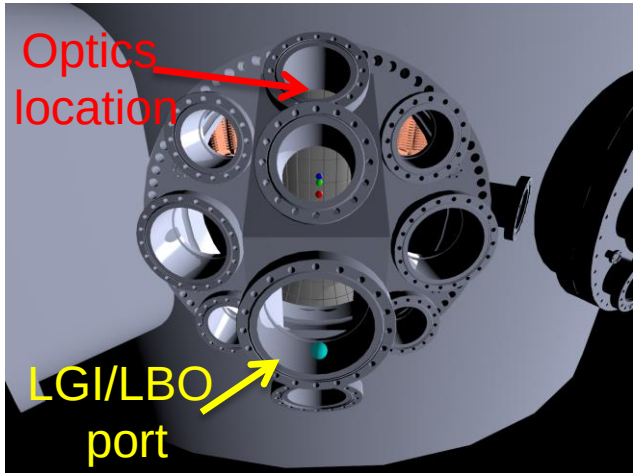

Private Gigabit links and automated acquisition allow full transfer of camera data within shot cycle

- Automated Labview acquisition synced with MDSPlus shot cycle
- Private Gigabit links for each camera to diagnostic room
  - Transfer to NSTX cluster via SMB mount up to 240 Mbs on 10Gbs switch
  - Recent tests with Globus allowed 960Mbs transfer speed from camera PCs with Gb NIC
  - Event-driven automated system for file transfer via Globus now being tested
- Real-time acquisition/analysis envisioned for radiative divertor control camera
  - On Gigabit based frame grabbing at most 30-50 Mpixel/s → 128x128, 2kHz, 8 bit
  - Upgrade to 10Gbs system for Phantom v1211 now under consideration
    - to allow ~200 Mpixel/s
  - FPGA-based system envisioned as a longer term upgrade

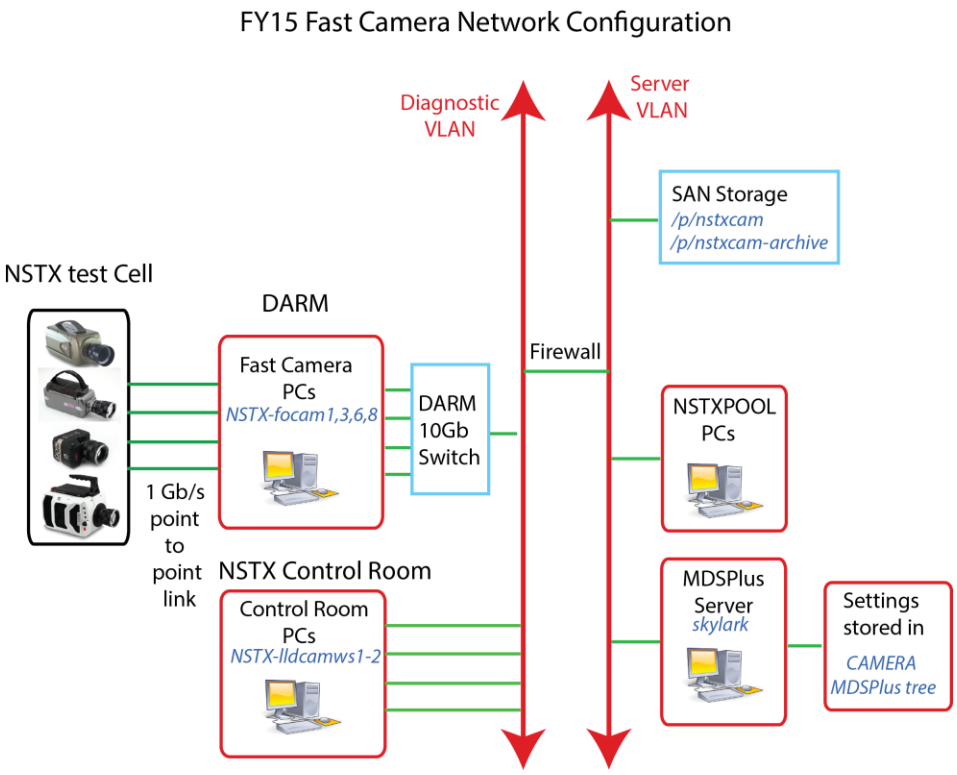

GigE Vision compliant frame grabber used for acquisition of analog CIDTEC cameras

- Analog RS-170 frame grabber (PCI-1408) now obsolete and not supported in Windows 7
- Pleora external frame-grabber successfully implemented for GigE Vision standard compliant digitization
  - Two analog inputs/frame grabber
- Private Gigabit links for each frame grabber to acquisition computer
- Automated Python acquisition synced with MDSPlus shot cycle
- Compact, USB-controlled oscilloscope and wave function generator controlled via Python for triggering of acquisition and intensifier gating control

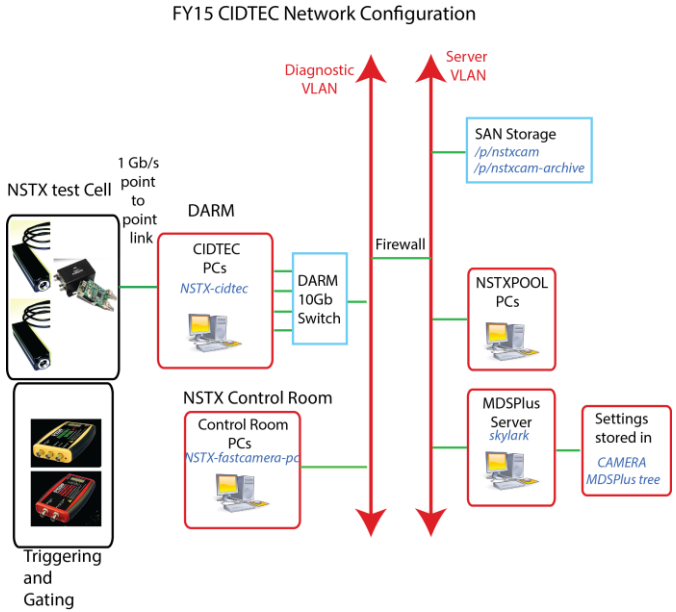

Evolution of impurity sources/sputtering in transition from boronization to lithium conditioning

- Evolution of C, B, Li, O sources with Li introduction and as Li accumulates in vessel not fully understood
  - Some reduction in C sputtering observed after large lithium deposition
  - Lithium sputtering consistent with physical and thermal sputtering from D-saturated surface
- Enhanced spectroscopic diagnostic suite to allow for full poloidal coverage and redundant, simultaneous measurements of impurity brightness from same charge states
- Experimental day dedicated to gradual introduction of lithium (led by R. Maingi)
- Characterization of B, C, Li, O sources/sputtering evolution:
  - After first lithium introduction, as a function of lithium dose, as lithium inventory builds up in the machine
- Evaluation of poloidal distribution and toroidal asymmetries (asymmetric lithium deposition) of impurity sources
- Attempt at carbon particle balance

Understand and characterize lithium coatings longevity, conditioning effectiveness

- NSTX developed empirical recipe for Li conditioning (dose, frequency of pre-discharge evaporation)
  - Observed divertor recycling, lithium sputtering evolution lifetime inconsistent with gross erosion only
  - What determines the observed lifetime?
    - Gross/net erosion, intercalation, reaction with background gases
- Understand experimentally-observed lithium coatings lifetime and develop a metric for lithium effectiveness based on PMI measurements to correlate with global parameters (led by F. Scotti)
- Deliverables to be compared with global parameters:
  - Local deuterium recycling (OSP, upper div, MAPP), Li, C, O sputtering (OSP, upper div., MAPP)
  - Gas pump-out rate, wall loading rate from deuterium particle balance
  - MAPP elemental composition
- Test effect of thickness/areal density, intercalation, reaction with background gases, evaporative coatings vs. plasma deposition

TWICE1 view dedicated to MAPP to connect surface science to spectroscopy and conditions at the OSP

- MAPP located in far SOL (R~100 cm)
  - Typical outer strike point, R~45-50 cm
  - ~100x difference in incident particle flux
- In FY16, 'non-destructive' MAPP capabilities :
  - XPS surface elemental composition (~5 nm) post-discharge
- TWICE1 view dedicated to MAPP monitoring during MAPP experiments with 2-color capabilities
- Goal: Relate post-exposure XPS elemental composition to material mixing from spectroscopy: C, Li, O sputtering, D retention
  - At MAPP-head,
  - Adjacent row 4 tiles
  - Outer strike point

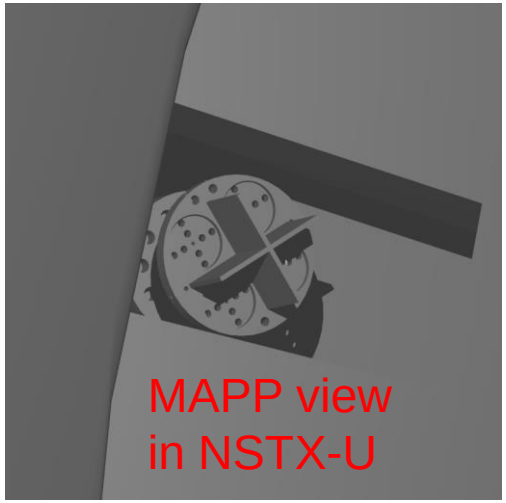

MAPP illuminated by vessel filament on LTX

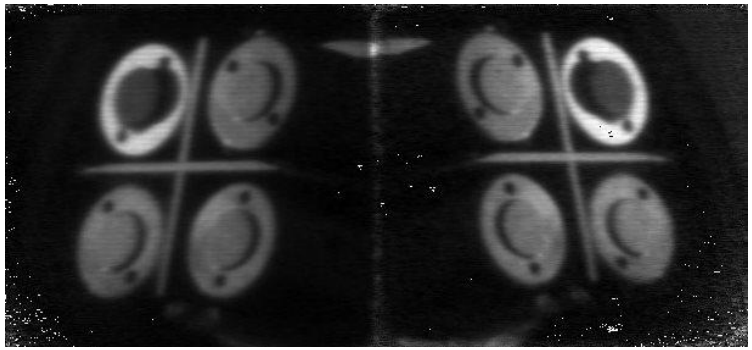

MAPP imaging on LTX

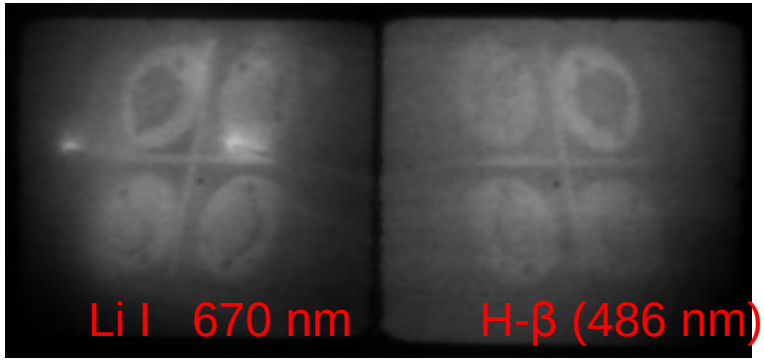

Establish optimal operation of new TMB system and characterize boronization effectiveness

- NSTX-U has a new D-TMP system:
  - Three D-TMB injection locations
  - D-TMB injected during He-GDC
- Experimental day to characterize/optimize new boronization system (led by C. Skinner)
  - Relate change in plasma performance to surface composition, uniformity of coatings via MAPP, QMBs, spectroscopy
- Spectroscopic imaging support via B II, B III monitoring

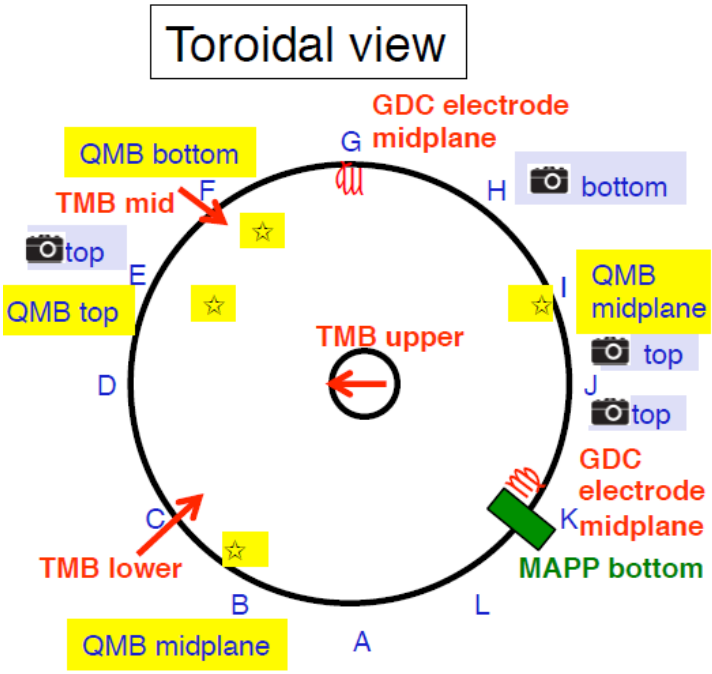

Summary

- Enhanced spectroscopic imaging diagnostic suite developed for NSTX-U to enable:
  - Full toroidal/poloidal coverage of impurity emission
  - Simultaneous measurements of impurity brightness from different atomic elements
  - Redundant measurements of impurity brightness from different wavelength of same impurity charge state
- Integration of wide angle fast camera views with higher resolution views on intensified CID cameras
- Support NSTX-U 2016 experimental campaign:
  - Characterization of boron-lithium transition
  - Optimization of boronization
  - Characterization of lithium coatings longevity
  - Characterization of divertor turbulent filaments

ENDD diagnostic updated with imaging bundle and new view aimed at NBI dump

- DALSA D256T camera
  - 128x128 pixels, up to 500 Hz
  - Schott imaging bundle, 4 ft 1000x800 fibers
- Dedicated to carbon sources monitoring and edge neutral density studies via DEGAS2

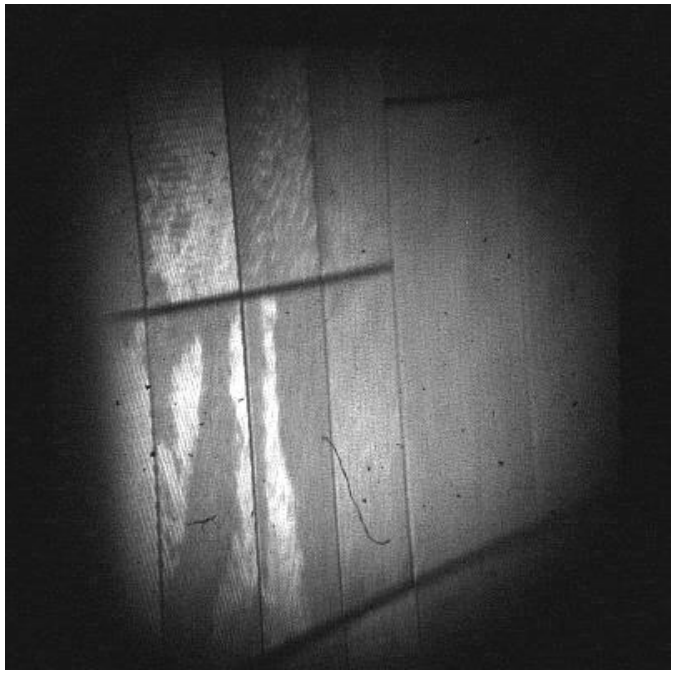

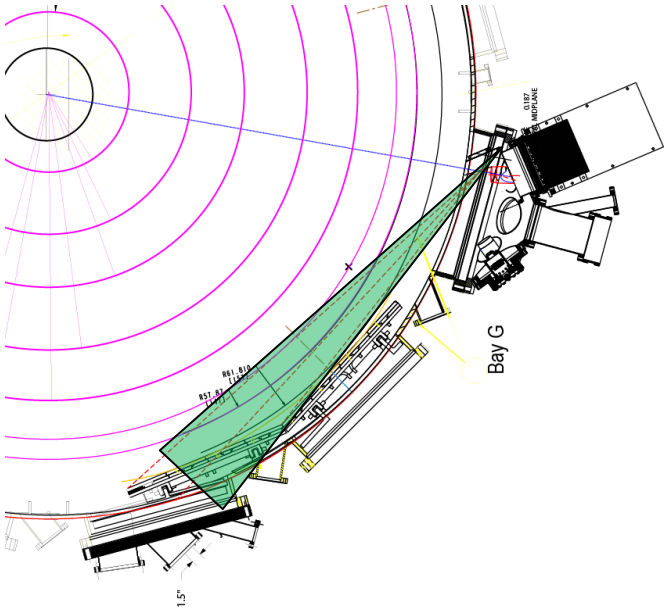

Remotely controlled filter wheels allow changing bandpass filters between discharges

- Filter wheels remotely controlled via RS-232 serial server and Velmex stepping motor connected to rotary stage
  - Allows bandpass filters change between discharges
- Filters included in filter wheels to support PMI and radiative divertor studies:
  - C I (909 nm), Gero band (430 nm), C II (514 nm, 723 nm), C III (465 nm), C IV (580 nm)
  - Li I (670 nm), Li II (548.5 nm), B III (449 nm)
  - D-alpha (656.1 nm), D-gamma (433.9 nm)
- Absolute calibration performed with Labsphere,
  - Post-run calibration in-situ after campaign